J Mol Model (2012) 18:2321–2331
DOI 10.1007/s00894-011-1254-6

ORIGINAL PAPER

Size and chain length effects on structural behaviors of biphenylcyclohexane-based liquid crystal nanoclusters by a coarse-grained model

Ming-Liang Liao · Shin-Pon Ju · Chun-Yi Chang · Wei-Lin Huang

Received: 11 May 2011 / Accepted: 21 September 2011 / Published online: 6 October 2011

Abstract Size and chain length effects on structural behaviors of liquid crystal nanoclusters were examined by a coarse-grained model and the configurational-bias Monte Carlo (CBMC) simulation. The nanoclusters investigated in this study are composed of the biphenylcyclohexane-based BCH5H liquid crystal molecule and its derivatives. Results of the study show that the average energy decreases (i.e., more negative) as the cluster size (i.e., the number of molecules) increases. With the increasing cluster size, the equilibrium conformation of the nanocluster changes gradually from a pipe-like structure (for the smaller systems) to a ball-like cluster (for the larger systems). The order parameter of the system reduces with the transition of the equilibrium conformation. Regarding the chain length effect, the pipe-like equilibrium conformation (for the smaller systems) was observed more close to a pipe as the length of the tail alkyl chain of the derivatives extended. However, due to the flexibility of the tail alkyl chain, the pipe conformation of the system deflects slightly about its cyclohexyl group as the tail extends further.

Keywords Effective potential energy · Equilibrium conformations · Moment of inertia · Order parameter

M.-L. Liao
Department of Aircraft Engineering,
Air Force Institute of Technology,
Kaohsiung 82047, Taiwan, Republic of China

S.-P. Ju (✉) · C.-Y. Chang · W.-L. Huang
Department of Mechanical and Electro-Mechanical Engineering,
National Sun-Yat-Sen University,
Kaohsiung 80424, Taiwan, Republic of China
e-mail: list1860@gmail.com

Introduction

Liquid crystals (LC) have been extensively applied in microdisplays [1] and focusing system [2]. For these applications, the main objective is to increase their optical efficiency. With recent advances in bio-technology, liquid crystals can also be used to reproduce the effects of naturally occurring lens systems [3–5]. The focal length of the lens is tuned by means of an electric field. As the voltage decreases, the liquid crystal lens has a shorter focal length. This application of liquid crystals could also lead to innovations in contact-lens materials.

To realize the possible applications of liquid crystals, the physical properties of liquid crystals have been extensively studied by experimental methods. For example, Holstein et al. [6] investigated the diffusion coefficient in nematic liquid crystals by the PFG-NMR. Gwag et al. [7] studied the polar anchoring energy between LC molecules and polyimide films and found the dependence of the pre-tilt angle of the liquid crystals on the orientation and thickness of the polyimide films. Somma et al. [8] explored the orientation molecular dynamics in oligofluorenes (OFs) by depolarized dynamic light scattering (DLS) and the dynamic NMR spectroscopy. Filpo et al. [9] examined the electro-optical and the morphological properties of reverse-mode polymer-dispersed liquid crystal (PDLC) films.

Although the steady-state of liquid crystals can be observed by experiments, there are some difficulties in the experimental methods. For instance, the detailed dynamic behavior of liquid crystals is hard to be inspected because of resolution limitations of the experimental equipment. The computer simulation methods could be used to retrieve the information beyond the experimental limitations and to provide dynamic behaviors of liquid crystals at an atomic level. Molecular dynamics (MD) simulation is a powerful

tool facilitating the investigation of detailed molecular behavior. As to this aspect, McDonald and Hanna [10] used the MD simulations to investigate the terrace of a liquid crystal fluid wetting on a surface. Capar and Cebe [11] examined the properties of liquid crystals for different alkyl chain lengths. Peláez and Wilson [12] performed MD simulations for a 2,5-bis-(p-hydroxyphenyl)-1,3,4-oxadiazole mesogen (ODBP-Ph-C_7) at various temperatures. Besides, Mirantsev and Virga [13] studied a nanoscopic nematic twist cell confined between two bounding substrates.

While the MD simulation is a powerful tool for investigation of detailed behaviors of liquid crystals, it is not efficient to perform over a long period of time to obtain long-period evolution of the liquid crystals. The problem is more significant for a system containing a large number of molecules. On this issue, many simplified methods have thus been developed. The coarse-grained method is one of the simplified methods commonly used for the analysis of liquid crystals. Regarding this method, many coarse-grained models have been utilized [14–17] to investigate behaviors of liquid crystals. For instance, Bates [14] adopted the bond fluctuation model to find the relation between the phase behavior and the stiffness of large flexible liquid crystals. Cifelli et al. [15] examined the order parameter and the diffusion coefficient of liquid crystals using the elementary liquid crystal model. Lin et al. [16] employed the rod-like molecular model to investigate the order parameter and phase behavior of lyotropic liquid crystal solution. In addition, Peter et al. [17] used the structure-based model to simulate liquid crystals having different densities. In our previous study [18], a coarse-grained model and the configurational-bias Monte Carlo simulation were also employed to obtain the orientational order parameter, the conformation of MMA-oligomers, and the substrate/MMA-oligomer interaction to realize effects of the interaction strength on the arrangement of MMA-oligomers. Results of the study demonstrated that the simulation method can be used successfully to obtain the structural behaviors of molecules.

In this study we extended the aforementioned method to investigate the structural behaviors of liquid crystal nanoclusters. Size and chain length effects on structural behaviors of liquid crystal nanoclusters were examined to understand variations in the equilibrium conformation of liquid crystal nanoclusters for various clusters sizes and chain lengths. The study could give some insights into the cluster size and chain length effects on structural behaviors of liquid crystal nanoclusters. This information is helpful for the design and applications of liquid crystal materials. This issue is of particular significance for investigating behaviors of mixtures consisting of different liquid crystal molecules. Mixing of two or more different compounds is a common procedure in liquid crystal science to tailor the material properties for attaining a specific phase or achieving materials with great anisotropy and low viscosity, which are important to many applications of the liquid crystal materials. This topic has arrested much attention in recent years. For example, Hong et al. [19] investigated the nature of molecular clustering in binary mixtures of bent-core (BC) and rod-shaped (RS) molecules and examined the influences of the concentration of RS compounds on the nanostructure of the binary mixtures. The nature of the tilted smectic clusters and related aspects of the nanostructure of the mixtures were also discussed in their research. Another application on mixing of liquid crystals is the method of doping commonly used in the liquid crystal science. For example, Wen et al. [20] utilized a non-polar liquid crystal compound as the dopant to liquid crystal mixtures for enhancing vertical alignment of the host liquid crystal mixtures. High-contrast vertical alignment of high birefringence liquid crystal mixtures were attained by their doping method.

Molecules of the liquid crystal nanoclusters investigated in this study are the biphenylcyclohexane-based (abbreviated as BCH) molecule and its derivatives. The reason that BCH molecules were examined in the study is owing to their many excellent features for applications in the liquid crystal display (LCD) devices. The BCH molecules have low viscosity and a high response speed. Because the terminal groups of BCH molecules are all alkyls, the dielectric anisotropy of the molecules is near zero. The non-polar BCH molecules can be used as a dopant to liquid crystal mixtures to enhance their vertical alignment. As a result, high-contrast vertical alignment of high birefringence liquid crystals can be obtained [20]. The application of the BCH dopant is very useful for developing high-contrast LCD devices such as large screen liquid crystal televisions. However, to the best of the authors' knowledge, there are not many related research works on structural behaviors of the BCH molecules. To attain some information on structural behaviors of these materials for their potential applications, the BCH molecules were analyzed in this paper.

The BCH molecules investigated in this study were selected as a compound of the 4,4′-disubstituted biphenylcyclohexane series (BCHRR') with R=C5H11 and R'=H, namely, the compound BCH5H. It has a molecular formula of H-C6H4-C6H4-C6H10-C5H11. Liquid crystal properties of bulk BCH5H have been examined by several experimental methods. A recent work of Muller and Haase [21] is an example. A coarse-grained model was employed to investigate cluster size and chain length effects on structural behaviors of liquid crystal nanoclusters composed of the BCH5H molecule and its derivatives. Potential energy, the order parameter, the moment of inertia, and equilibrium conformations of the nanoclusters were all examined in the

study. To explore the size effect on the structural behaviors, various nanoclusters (each consisting of the same molecule but with a different number of molecules) were considered. The chain length effect was examined by varying the number of carbon atoms in the R group of the biphenylcyclohexane series BCHRR', namely, by considering the derivatives of the BCH5H molecule.

Simulation methods

A coarse-grained model and the Monte Carlo simulation were employed in this research. A linked-vector model similar to that adopted by Clancy [22] was chosen as the coarse-grained model. The configurational-bias Monte Carlo simulation (CBMC) algorithm [23] was employed for the molecular simulations. The following is a brief description of the simulation method.

A coarse-grained model: the linked-vector model

For ease of discussion, the coarse-grained linked-vector model of a BCH5H molecule was shown in Fig. 1. The molecule was simplified by dividing it into five coarse-grained (CG) units along its backbone and modeled as a series of vectors linked at the terminals of the CG units. The molecule was thus simplified as a coarse-grained chain. A bead was placed at the midpoint of each linked vector and was used as the site for calculating the nonbonding interaction energy between two non-successive beads in the same chain and between beads on different chains. As shown in the figure, beads 1 and 2 represent the two phenyl groups of the molecule, bead 3 means the cyclohexyl group, and beads 4 and 5 stand for the tail alkyl chain. The bonding intramolecular interaction between two successive CG units was determined by probability distributions of the lengths and angles of the linked vectors. These probability distributions were obtained from the fully atomistic MD simulation of the molecule with the aid of the ENCAD force field [24] and were applied to the configurational-bias Monte Carlo simulation.

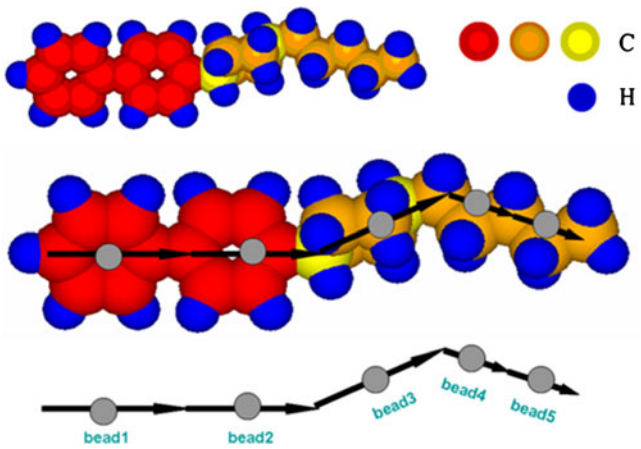

Fig. 1 The linked-vector model of a BCH5H molecule

Calculation of the nonbonding interaction energy is important for coarse-grained modeling. In this study, the continuous spherically-symmetric effective potential energy, U_{eff}, was employed to calculate the nonbonding interaction energy, which can be written as [22]

$$U_{eff}(r,T) = -k_B T \ln\left\langle e^{-\beta U'}\right\rangle, \tag{1}$$

where r is the distance between two beads of the linked-vector model, T the system temperature, k_B the Boltzmann constant, U' the potential energy, and $\beta=1/(k_BT)$. The angled bracket pair in Eq. 1 represents the angular average for a fixed value of r. The potential energy U' is determined from the nonbonding interaction of the fully atomistic model of CG units by using the ENCAD force field, which can be expressed by

$$U' = U_{vdw} + U_{els}, \tag{2}$$

where U_{vdw} is the van der Waals energy and U_{els} is the electrostatic energy. They have the following forms [24]

$$U_{vdw} = \sum_{i,j}\left[A_{sc}\varepsilon^{ij}\left(r_0^{ij}/r_{ij}\right)^{12} - 2\varepsilon^{ij}\left(r_0^{ij}/r_{ij}\right)^{6} - S_{vdw}(r_{ij})\right], \tag{3}$$

$$U_{els} = \sum_{i,j}\left[q^i q^j/r_{ij} - S_{els}(r_{ij})\right], \tag{4}$$

where r_{ij} indicates the distance between nonbonding atoms i and j, A_{sc} is used to compensate for the interaction lost at small cutoff distances, and q^i and q^j stand for the partial charges of atoms i and j, respectively. The energy parameter (ε^{ij}), the distance parameter (r_0^{ij}), the partial charges (q^i and q^j), and the truncation shift functions (S_{vdw} and S_{els}) can be found from the ENCAD force field [24]. In this research, the cutoff distance was selected as 9 Å and the value for A_{sc} was specified as 0.84. It should be noted that the choice of the parameter A_{sc} is dependent on the cutoff distance because it is used to reduce the van der Waals repulsion to compensate for the reduced attraction caused by truncation (i.e., by the use of the cutoff distance). An optimum value of 0.84, which was commonly used in investigation of proteins and nucleic acids system [24], was also employed in this paper.

The effective potential energy with respect to the bead distance for the linked-vector model of BCH5H (Fig. 1) is shown in Fig. 2. For ease of representation, only the potential energy for part of the beads was displayed. It is evident from Fig. 2a that the interaction between bead 1 and bead 3 is apparently stronger than that between bead 1

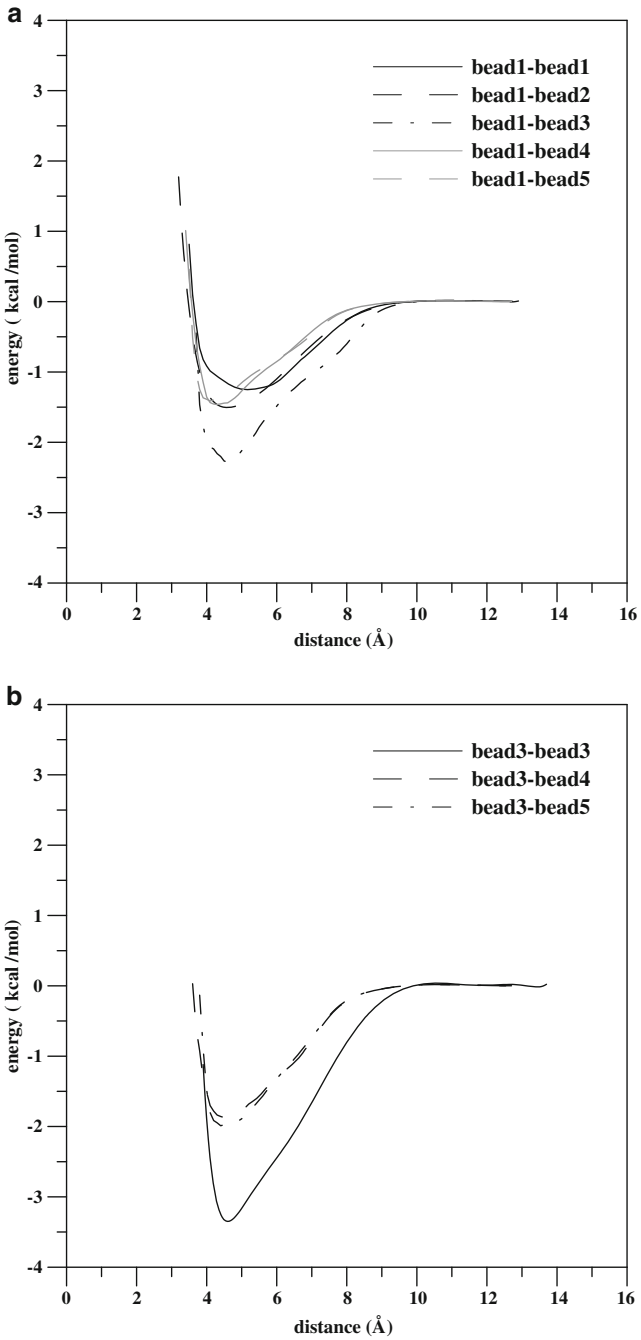

Fig. 2 Effective potential energy for the BCH5H model: (**a**) energy between bead 1 and each bead; (**b**) energy between bead 3 and beads 3, 4, and 5

and other beads. Since bead 3 (representing the cyclohexyl group in BCH5H) contains the largest number of atoms as compared to other beads, the interactions including bead 3 are larger than those between other pairs. Thus, the interaction between bead 3 and bead 3 (from a different chain) is largest, as can be seen from Fig. 2b where the strongest attraction was observed to occur at a bead distance of about 4.8 Å.

The configurational-bias Monte Carlo simulation

The configurational-bias Monte Carlo (CBMC) simulation is a molecular simulation technique commonly used to obtain an equilibrium conformation of polymers. In CBMC simulations, the Rosenbluth weight factor is used to bias the acceptance of the trial conformations generated by the Rosenbluth procedure [23]. This process guarantees that all chain conformations are generated with the correct Boltzmann weight and makes it more efficient than the traditional Monte Carlo simulation methods for the simulation of long-chain molecules [25].

In the present study, the CBMC algorithm was applied on the linked-vector model described above to obtain equilibrium conformations of the nanoclusters. The molecules studied were placed in a large vacuum space and no periodic boundary conditions were applied to the system. Initially, all chains of the simulation system were arranged in a regular pattern, packed chain by chain with their molecular long axes aligned. As an example, Fig. 3 shows the initial conformation for a BCH5H nanocluster with the number of chains $m=15$. Each chain was described by the same colored linked balls, which were used to represent the end points of the linked vectors. The linked vectors of all coarse-grained chains were then moved vector by vector via the CBMC algorithm [23] until the conformation corresponding to an energetically favorable state (i.e., the equilibrium conformation) had been attained.

To gain some information about structural behaviors of the liquid crystal nanoclusters at low temperatures, the system temperature of each case studied in this paper was set to be 50 K. Low-temperature behaviors of liquid crystals are of significance for comprehending the detailed characteristics of their crystalline state. Up to date, to the authors' knowledge, not many related works were found in the available literature. Recently, Bezrodna et al. [26] studied photoluminescence spectra of the 4-n-pentyl-4′-cyanobiphenyl (5CB) liquid crystal at low temperatures ranging from 4.2 to 200 K. Several crystal modifications of

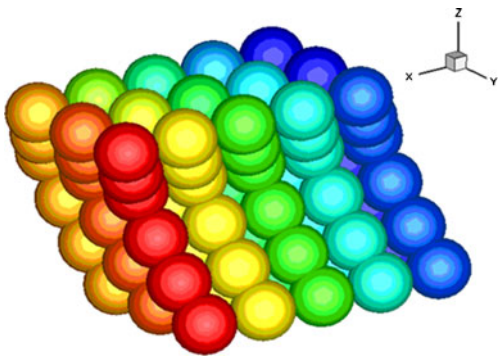

Fig. 3 Initial conformation for a BCH5H nanocluster with number of chains $m=15$

5CB, having different 5CB monomer and dimer conformers, were observed below 160 K. The simultaneous co-existence of the different conformers of the 5CB molecules at the low temperatures is responsible for the formation of the different types of monomer and dimer structures. Although at the temperature (50 K) of the present study, owing to the kinetics of crystal formation at the low temperature, the BCH5H liquid crystal might finally approach a crystalline phase in bulk state if the simulation time is sufficiently long, phase transition behaviors and bulk properties of the liquid crystal were not examined in the study. It is an interesting topic worthy for future studies and needs more efforts to discuss. Besides this topic, low-temperature structural behaviors of liquid crystal nanoclusters are also worthy to investigate. Investigation of low-temperature structural behaviors of nanoclusters composed of the BCH5H molecule and its derivatives is helpful for understanding the low-temperature variations in orientational ordering, molecule morphology, and the cluster shape with respect to the changes in the cluster size and molecule chain length. Information from the investigation is useful for characterization of conformation changes and molecular alignments for the systems containing the BCH5H related molecules. This is beneficial to the applications of the molecules, especially in the mixing and doping methods for modifications of liquid crystal mixtures containing the molecules.

To avoid achieving conformations corresponding to local minimal energy of the simulation system and to assure the actual equilibrium conformation of the system was obtained, a simulated annealing method [27] was applied to the simulation. During the simulation, the nanocluster was annealed from the room temperature (T=300 K) to the target temperature (T=50 K) with a decreasing rate of 50 K per 3×10^5 CBMC steps. When the system reached the target temperature, a total number of 2×10^6 CBMC steps were continued, which were demonstrated to be sufficient for the equilibrium conformation of the system. One step in the CBMC simulation denotes one trial move on all the linked vectors of the system. The equilibration of the system was assured if the energy of the nanocluster converges to a stable value. The total number of simulation steps (2×10^6) was noticed to be sufficient for the equilibration of the studied cases because deviations in the energy are all less than 2%. Data from the last 1000 steps were averaged to examine the structural behaviors of the nanocluster.

Results and discussion

Structural behaviors of liquid crystal nanoclusters composed of the BCH5H molecule and its derivatives were investigated in this study. Cluster size and chain length effects on the structural behaviors were examined by inspecting the order parameter, the potential energy, the moment of inertia, and equilibrium conformations of the nanoclusters. Results of the simulations are discussed as follows.

The BCH5H molecule

Figure 4 shows the average energy and order parameter for BCH5H nanoclusters, each containing a different number of BCH5H molecules. Since each molecule of the system was modeled by a coarse-grained chain, the size effect on structural behaviors of the nanoclusters can be observed from the influence of the number of chains (i.e., the cluster size). To examine the size effect on the interaction between BCH5H molecules, only the nonbonding interaction energy was shown in Fig. 4. This energy was calculated from the contributions of the van der Waals energy and the electrostatic energy. It corresponds to the interaction strength between the BCH5H molecules.

Since the energy in Fig. 4 is negative, the interaction between BCH5H molecules is attraction dominant. The average energy was noticed to decrease (i.e., more negative) as the number of chains m of the cluster size grows. When the number of chains is greater than 75, the average energy tends to approach a constant value. This indicates that for the nanocluster with m larger than 75, the average energy of molecules approaches to that of bulk BCH5H. This is because in a system with attractive interactions the interfacial molecules have higher energy (i.e., less negative) than the inner molecules of the cluster.

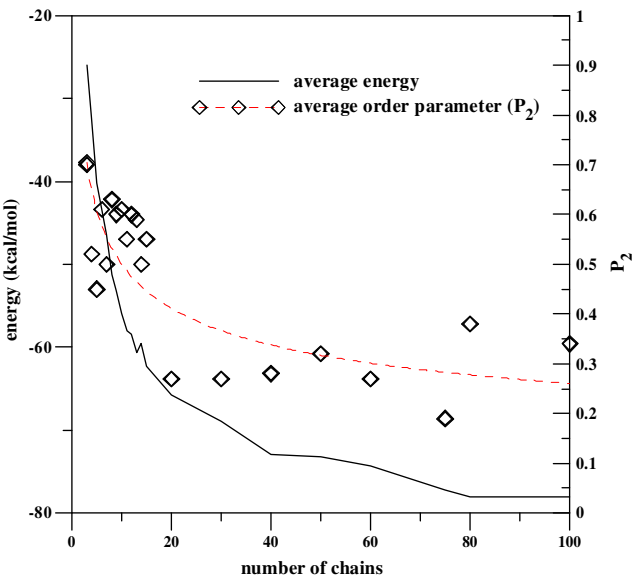

Fig. 4 The average energy and order parameter P_2 for the BCH5H nanoclusters with various numbers of chains

As the cluster size increases, because of the decrease in the ratio of interfacial molecules to inner molecules, the average energy decreases (i.e., more negative) and reaches a constant value corresponding to the bulk value. Similar behaviors could also be found in the study of size effects on the molecular behavior of a water nanocluster [28].

The order parameter P_2 in Fig. 4 was determined by [11]

$$P_2 = \frac{3\langle \cos^2\theta \rangle - 1}{2}, \tag{5}$$

where P_2 is the second-rank order parameter commonly used in the analysis of liquid crystals, and the value for $\cos\theta$ is written as

$$\cos\theta = \mathbf{u} \cdot \mathbf{n}, \tag{6}$$

where **u** is a unit vector representing the long axis direction of a certain molecule in the nanocluster and can be calculated from the eigenvector corresponding to the smallest eigenvalue of the moment of the inertia tensor for the specific molecule. The unit vector **n** stands for the director of the nanocluster and can be found by diagonalizing a second-rank ordering tensor **Q** of the system [11]. The angled bracket pair used in Eq. 5 denotes the ensemble and time average. From definition of the order parameter, Eq. 6, the molecules form a disordered conformation when P_2 approaches to zero, whereas they align with a common director (i.e., form a more ordered conformation) as P_2 approaches unity.

From Fig. 4, the order parameters of the nanoclusters were seen not to have monotonous dependence upon the cluster size. However, it tends to decrease, on average, with an increase in the number of chains (m). For nanoclusters with fewer molecules, the molecules were observed to arrange in a more ordered manner than those with a larger cluster size. The non-monotonous dependence of the order parameter, especially for $m<15$, might be ascribed to the fewer molecules sampled in the calculation of the average order parameter.

Figure 5 displays the equilibrium conformations for the BCH5H nanoclusters with the number of chains m=3, 6, 10, and 15. It was noticed that for the nanoclusters with fewer molecules (m=3 and 6), the equilibrium conformations exhibit a pipe-like structure and the molecules seem to intertwine along the pipe axis. The intertwining of the molecules is due to the stronger intermolecular attraction from the cyclohexyl group (bead 3), shown in Fig. 2. Because the tail alkyl chain (beads 4 and 5) is more flexible than the phenyl group (beads 1 and 2), a large bending angle between beads 3 and 4 is thus formed owing to the stronger attraction. The large bending angle causes the molecules to more easily intertwine along the pipe axis. It should be noted that the intertwining-pipe structure is formed to reduce the surface area of the nanocluster and to obtain a more stable configuration. This behavior can also be observed in our previous studies about gold nanowires, which also exhibit helical structures when the diameters of the gold nanowires are smaller than 1 nm [29, 30].

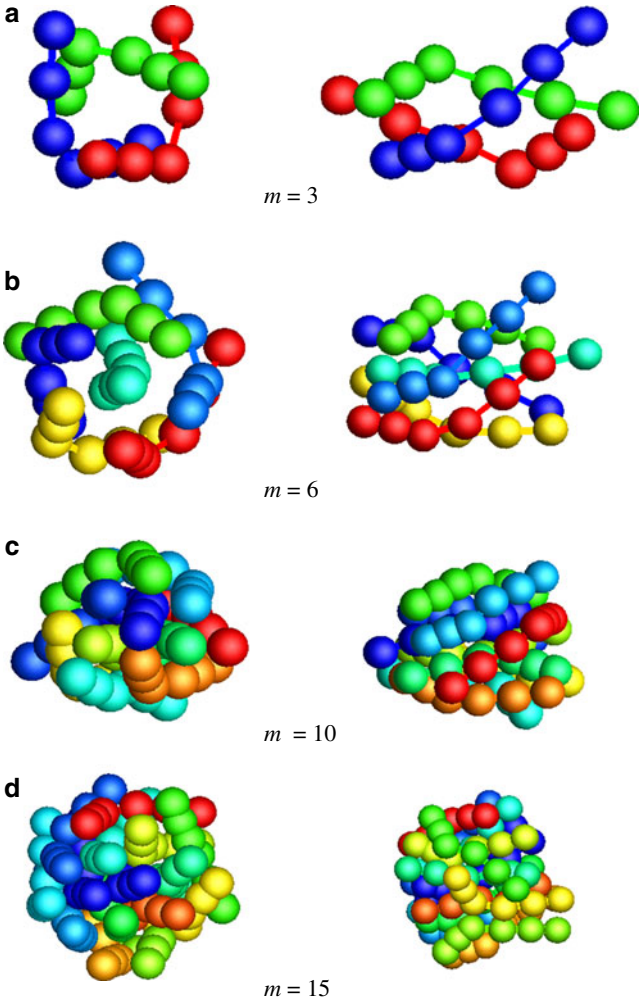

Fig. 5 Equilibrium conformations for the BCH5H nanoclusters with (**a**) m=3, (**b**) m=6, (**c**) m=10, and (**d**) m=15 (m: number of molecules). The left shows the front view and the right shows the side view of the conformations

As the cluster size increases, the molecules tend to fill with the hollow space of the pipe and a ball-like equilibrium conformation is formed gradually, as can be seen from Fig. 5d. The transition from a pipe-like conformation to a ball-like conformation, when the number of molecules grows, results in the decrease in the average energy as discussed in Fig. 4. This transition also induces a reduction in the arrangement order of the molecules and thus reduces the order parameter of the nanocluster (cf. Fig. 4). The transition of the cluster shape might be ascribed to the increase in interfacial tension (i.e., surface tension) of the nanocluster. As the cluster size enlarges, the interfacial tension makes the nanocluster reduce its surface area by adopting a spherical shape. This leads to the ball-

like conformation in the large system, as shown in Fig. 5d. However, when the nanocluster is too small (i.e., consisting of a few molecules) this shape cannot be adopted without sacrificing intermolecular contacts. Moreover, the surface tension decreases largely for the small system and it cannot support the spherical shape. Therefore the nanocluster does not form a ball-like shape but rather tries to adjust its shape to a more stable elongated shape, i.e., the pipe-like conformation as shown in Fig. 5a. This phenomenon also exists in size effects on the molecular behaviors of a water nanocluster [28].

The transition of the equilibrium conformations can also be demonstrated by inspecting ratios of three quantities, relating to the moment of inertia of the nanocluster i.e., g_2/g_1 and g_3/g_1 [31]. The quantities g_1, g_2, and g_3 designate the maximum, medium, and minimum eigenvalues, respectively, of a 3×3 matrix G with component $G_{\alpha\beta}$ calculated by [31]

$$G_{\alpha\beta} = \left\langle \sum_{i=1}^{n} m_i (r_{i\alpha} - r_{c\alpha})(r_{i\beta} - r_{c\beta}) \right\rangle \qquad \alpha,\beta=x,y,z, \tag{7}$$

where m_i and $r_{i\alpha}$ are the mass and position of the coarse-grained bead i in the sampled molecule, respectively; $r_{c\alpha}$ means the position of the center of mass of the nanocluster. The summation is carried out over all coarse-grained beads of the sampled molecule and n is the number of linked vectors (coarse-grained beads) of the nanocluster. It should be noted that the sum of g_1, g_2, and g_3 is just equal to the mean-square radius of gyration of the nanocluster. The ratios g_2/g_1 and g_3/g_1 of a nanocluster can provide information about the conformation of the nanocluster. If both of them approach unity, it means that the nanocluster has a spherical or ball-like conformation. If their values are nearly the same value but far from unity, it implies that the nanocluster has a rod-like or pipe-like conformation.

Figure 6 shows the ratios g_2/g_1 and g_3/g_1 for the BCH5H nanoclusters with various cluster sizes. As can be seen from the figure, the ratios are nearly the same and far from unity as the number of chains m is below six. It means that the equilibrium conformation of the smaller nanocluster (with m<6) exhibits a pipe-like structure. This corresponds to the conformations displayed in Fig. 5a and b. The ratios were also observed to rise rapidly and approach unity with the increase of the cluster size. This implies, for the nanocluster with a greater number of molecules, its equilibrium conformation tends to a sphere or a ball. Figure 5c and d shows the transition from the pipe-like conformation to the ball-like conformation.

The ball-like equilibrium conformation is more evident for the nanocluster with m=100, as can be observed from Fig. 7. The ratios g_2/g_1 and g_3/g_1 for the nanocluster are

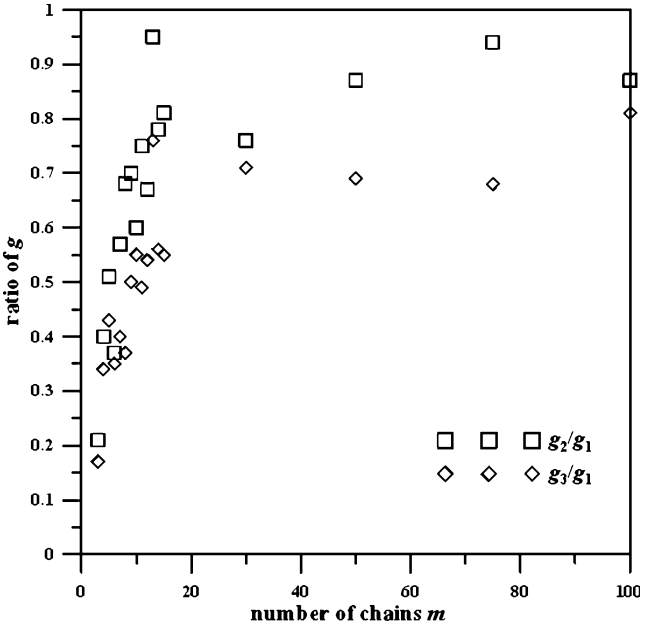

Fig. 6 Ratios of g_2/g_1 and g_3/g_1 for the BCH5H nanoclusters with various numbers of chains

0.87 and 0.81, respectively, which demonstrates the near spherical conformation for the nanocluster. The helical behavior in the smaller nanocluster (with m<6) does not appear in this case. Although the variations in the order parameter and the g_2/g_1 and g_3/g_1 ratios are fluctuating and not monotonous (as can be seen from Figs. 4 and 6), on average, the tendency of the conformational change from a pipe-like to a ball-like conformation as the number of molecules (m) increases can be observed from Fig. 6. The slightly increasing order parameter for m=80 and 100 (shown in Fig. 4) might be ascribed to the somewhat regular arrangement of the molecules in the ball-like conformation (as shown in the circle area of Fig. 7). Because the order parameter increases only slightly, the

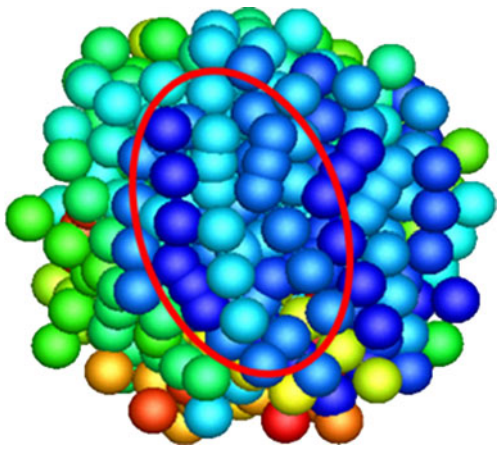

Fig. 7 Equilibrium conformations for the BCH5H nanoclusters with m=100

pipe-like conformation existing in small nanoclusters does not appear in the spherical cluster.

Derivatives of the BCH5H molecule

The chain length effect was investigated by considering structural behaviors of the BCH5H molecule and its derivatives. To discuss the chain length effect, the derivatives were selected by varying the number of carbon atoms in the R group of the biphenylcyclohexane series BCHRR'. In this work we compared the structural behaviors of molecules with R=C_3H_7, C_5H_{11} (i.e., BCH5H), C_7H_{15}, and $C_{11}H_{23}$, remaining R' unchanged (i.e., R'=H). Similar to the coarse-grained modeling for the BCH5H molecule, the molecules were modeled by linked vectors with various repeated tail units, as shown in Fig. 8. The number of linked vectors n used in the models is four, five, six, and eight for R=C_3H_7, C_5H_{11}, C_7H_{15}, and $C_{11}H_{23}$, respectively. Since only the number of the repeated linked vectors was altered, the effective potential energy calculated for the BCH5H molecule can also be applied to the CBMC simulation method.

The size effect on the structural behaviors of the molecules with various tail lengths was observed to be similar to that on the structural behaviors of the BCH5H molecules. As the cluster size (i.e., the number of molecules m) grows, the average energy decreases and the equilibrium conformation of the nanocluster changes from a pipe-like to a ball-like structure. As a result, the order parameter P_2 of the nanocluster decreases with the increase of the cluster size.

The pipe-like structure of the smaller nanocluster is of special interest in this study. We examined effects of the tail length on the conformation of the smaller nanocluster. Figure 9 shows the equilibrium conformations for the nanoclusters with the number of molecules m=6 and various numbers of linked vectors n. The pipe-like conformations for the smaller nanoclusters were noticed from the figure. The intertwining of the molecules due to

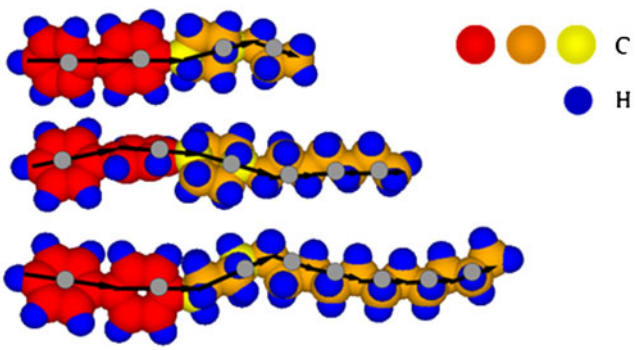

Fig. 8 The linked-vector model of derivatives of the BCH5H molecule with n=4, 6, 8, respectively

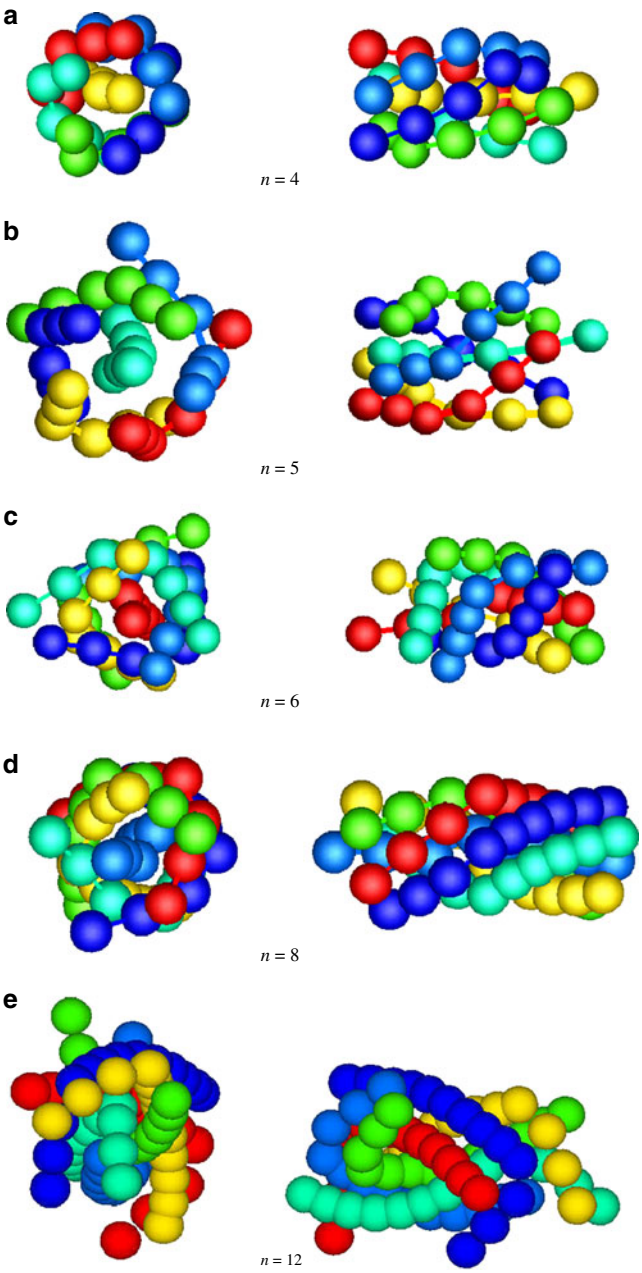

Fig. 9 Equilibrium conformations for the nanoclusters with m=6 and various chain lengths (**a**) n=4, (**b**) n=5, (**c**) n=6, (**d**) n=8, and (**e**) n=12 (n: number of linked vectors). The left shows the front view and the right shows the side view of the conformations

the stronger intermolecular attraction from the cyclohexyl group (bead 3) was also observed. The intertwining behavior is more evident for the nanocluster with n=6. This leads to the apparent reduction in the order parameter P_2 of that nanocluster, as can be seen from Table 1.

Table 1 also lists the ratios of g_2/g_1 and g_3/g_1 for the nanoclusters with various tail lengths. It was noted that the ratios g_2/g_1 and g_3/g_1 for the nanocluster with n=8 are lower than those of the other nanoclusters. The obvious decrease in the ratios causes the equilibrium conformation

Table 1 Properties for the nanoclusters with the number of molecules m =6 and various tail lengths

Number of linked vectors (n)	g_2/g_1	g_3/g_1	Order parameter (P_2)
4	0.40	0.37	0.70
5	0.37	0.35	0.61
6	0.42	0.34	0.46
8	0.20	0.18	0.73
12	0.19	0.30	0.49

of the nanocluster to be closer to a pipe structure as compared with that of the others, shown in Fig. 9d. The pipe structure also results in the evident rise in the order parameter of the nanocluster as can be seen from Table 1. The tendency to form a more pipe-like equilibrium conformation is ascribed to the increasing attraction between the tail alkyl chains of the molecules. When the attraction between the tail alkyl chains is greater than that from the cyclohexyl group, the tail alkyl chains tend to intertwine themselves. The nanocluster hence has a more pipe-like equilibrium conformation. To demonstrate this relation, Fig. 10 shows the interaction energy between the tail alkyl chains and between the cyclohexyl group (bead 3) and the tail alkyl chain for (a) n=5 and (b) n=8. As shown in the figure, the attraction between the tail alkyl chains is much greater than that between the cyclohexyl group and the tail alkyl chain for n=8 as compared with the case for n=5. The nanocluster with n=8 thus has a more pipe-like equilibrium conformation.

It could be observed from Fig. 9e that as the tail alkyl chain extends further (for n=12), the pipe conformation of the nanocluster deflects slightly about its cyclohexyl group. This may be attributed to the flexibility of the tail alkyl chain as the tail extends further. Owing to this deflection, the order parameter of the nanocluster reduces as can be seen from Table 1. The intertwining and deflecting behaviors of the molecules might be the main reason for the variations in the order parameter. Sensitive fluctuation due to small sampling data might be another reason.

Conclusions

Size and chain length effects on structural behaviors of nanoclusters composed of the BCH5H molecule and its derivatives have been investigated by a coarse-grained model and the configurational-bias Monte Carlo (CBMC) simulation. The molecule was modeled as a series of successive coarse-grained linked vectors along the backbone of the molecule. The ENCAD force field was utilized to calculate the effective potential energy of the coarse-grained model which was applied to the CBMC simulation. Structural behaviors of the nanoclusters were examined by inspecting the nonbonding potential energy, the order parameter, the moment of inertia, and equilibrium conformations of the nanoclusters. The size effect on the structural behaviors was explored by considering the BCH5H nanoclusters consisting of various numbers of molecules. The chain length effect was examined by

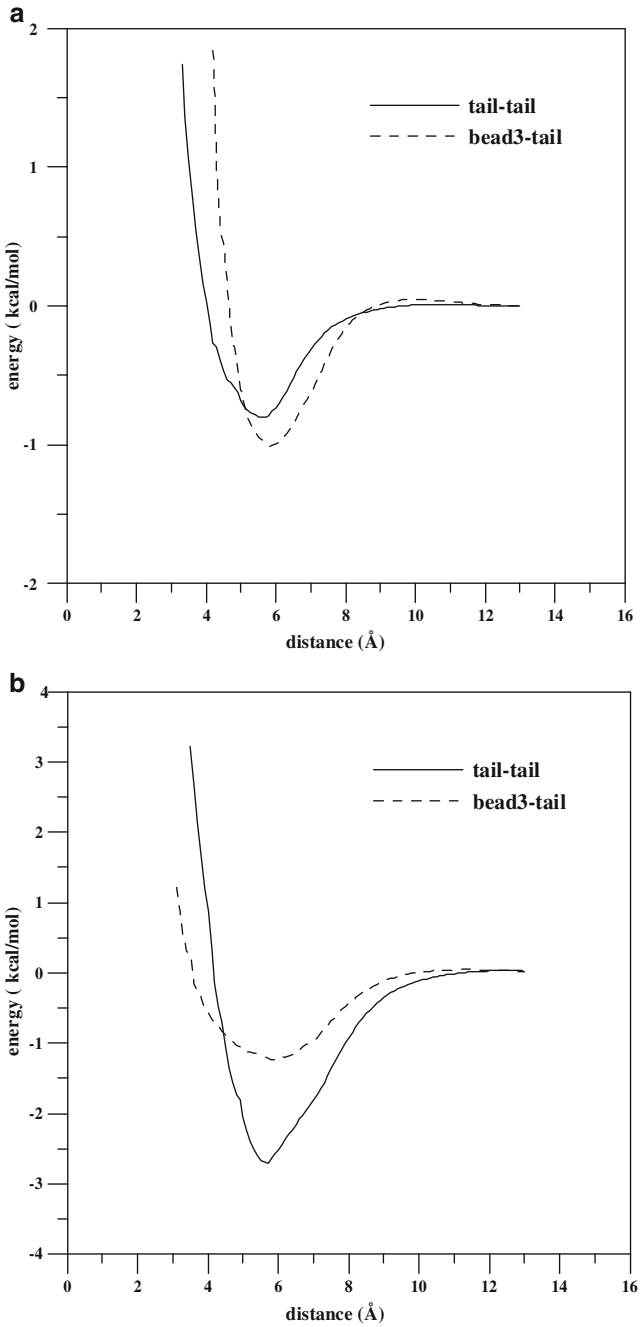

Fig. 10 Interaction energy between the tail alkyl chains and between the cyclohexyl group and the tail alkyl chain for (**a**) n=5 and (**b**) n=8

extending the tail alkyl chain of the BCH5H molecule, i.e., by analyzing the derivatives of the BCH5H molecule.

From the results of this study, the average energy was noticed to decrease (i.e., more negative) with the enlargement of the cluster size, namely, with the increase of the number of molecules (m) in the nanocluster. With the increasing cluster size, the equilibrium conformation of the BCH5H nanocluster changes gradually from a pipe-like structure (for the smaller systems) to a ball-like structure (for the larger systems). The order parameter of the nanocluster decreases with the transition of the equilibrium conformation. For the nanocluster with $m=100$, a near spherical equilibrium conformation was observed.

The cluster size was noted to have similar effects on the structural behaviors of the derivatives of the BCH5H molecule. Regarding the chain length effect, the pipe-like equilibrium conformation (for the smaller systems) was found more close to a pipe as the length of the tail alkyl chain of the derivatives enlarged. However, owing to the flexibility of the tail alkyl chain, the pipe conformation of the nanocluster deflects slightly about its cyclohexyl group as the tail extends further (for $n=12$).

Acknowledgments The authors gratefully acknowledge the support provided to this study by the National Science Council of the Republic of China under Project Grant No. NSC 96-2221-E-344-003 and NSC96-2628-E-110-005-MY2. The authors also thank the editor and referees for their helpful recommendations to make this paper more readable.

References

1. Zhang B, Li K, Chigrinov VG, Kwok HS, Huang HC (2005) Application of photoalignment technology to liquid-crystal-on-silicon microdisplays. Jap J Appl Phys 44:3983–3991. doi:10.1143/JJAP.44.3983
2. Mao YE, Wang B, Takahashi T, Sato S (2007) Properties of variable-focus liquid crystal lens and its application in focusing system. Opt Rev 14:173–175. doi:10.1007/s10043-007-0173-3
3. Ren H, Fan YH, Wu ST (2004) Liquid-crystal microlens arrays using patterned polymer networks. Opt Lett 29:1608–1610. doi:10.1364/OL.29.001608
4. Cheng CC, Chang CA, Yeh JA (2006) Variable focus dielectric liquid droplet lens. Opt Expr 14:4101–4106. doi:10.1364/OE.14.004101
5. Woltman SJ, Jay GD, Crawford GP (2007) Liquid crystal materials find a new order in biomedical applications. Nat Mater 6:929–938. doi:10.1038/nmat2010
6. Holstein P, Bender M, Galvosas P, Geschke D, Kärger J (2000) Anisotropic diffusion in a nematic liquid crystal— An electric field PFG NMR approach. J Mag Res 143:427–430. doi:10.1006/jmre.2000.2028
7. Gwag JS, Kim JC, Yoon TH, Cho SJ (2006) Effect of polyimide layer surfaceson pretilt angles and polar anchoring energy of liquid crystals. J Appl Phys 100:093502. doi:10.1063/1.2372229
8. Somma E, Chi C, Loppinet B, Grinshtein J, Graf R, Fytas G, Spiess HW, Wegner G (2006) Orientation dynamics in isotropic phases of model oligofluorenes: Glass or liquid crystal. J Chem Phys 124:204910. doi:10.1063/1.2191059
9. Filpo GD, Cassano R, Tortora L, Nicoletta FP, Chidichimo G (2008) UV tuning of the electro-optical and morphology properties in polymer-dispersed liquid crystals. Liq Crys 35:45–48. doi:10.1080/02678290701769915
10. McDonald AJ, Hanna S (2004) Atomistic computer simulations of terraced wetting of model 8CB molecules at crystal surfaces. Mol Crys Liq Crys 413:135–144. doi:10.1080/15421400490437222
11. Capar MI, Cebe E (2006) Molecular dynamics study of the odd-even effect in some 4-n-alkyl-4'-cyanobiphenyls. Phys Rev E 73:061711. doi:10.1103/PhysRevE.73.061711
12. Peláez J, Wilson MR (2006) Atomistic simulations of a thermotropic biaxial liquid crystal. Phys Rev Lett 97:267801. doi:10.1103/PhysRevLett.97.267801
13. Mirantsev LV, Virga EG (2007) Molecular dynamics simulation of nanoscopic nematic twist cell. Phys Rev E 76:021703. doi:10.1103/PhysRevE.76.021703
14. Bates MA (2004) Coarse grained models for flexible liquid crystals: parameterization of thebond fluctuation model. J Chem Phys 120:2026. doi:10.1063/1.1634551
15. Cifelli M, Cinacchi G, Gaetani LD (2006) Smectic order parameters from diffusion data. J Chem Phys 125:164912. doi:10.1063/1.2359428
16. Lin S, Numasawa N, Nose T, Lin J (2007) Coarse-grained molecular dynamics simulations for lyotropic liquid-crystalline solutions of semiflexible rod-like molecules. Mol Crys Liq Crys 466:53–76. doi:10.1080/15421400701246309
17. Peter C, Site LD, Kremer K (2008) Classical simulations from the atomistic to the mesoscale and back: coarse graining an azobenzene liquid crystal. Soft Matter 4:859–869. doi:10.1039/B717324E
18. Chang CY, Ju SP (2010) Investigation of methyl methacrylate-oligomer adsorbed on grooved substrate of different aspect ratios by coarse-grained configurational-bias Monte Carlo simulation. J Chem Phys 133:144710. doi:10.1063/1.3489661
19. Hong SH, Verduzco R, Gleeson JT, Sprunt S, Jákli A (2011) Nanostructures of liquid crystal phases in mixtures of bent-core and rod-shaped molecules. Phys Rev E 83:061702. doi:10.1103/PhysRevE.83.061702
20. Wen CH, Wu B, Gauza S, Nie X, Wu ST (2006) Dopant-enhanced vertical alignment of negative liquid crystals. Mol Cryst Liq Cryst 454:315–324. doi:10.1080/15421400600655949
21. Muller HJ, Haase W (2004) Refractive indices, density and order parameters for some Biphenl cyclohexanes. Mol Crys Liq Crys 409:127–135. doi:10.1080/15421400490430887
22. Clancy TC (2004) A novel approach to the regioselective synthesis of a disulfide-linked heterodimeric bicyclic bicyclic peptide mimetic of brain-derived neurotropic factor. Polymer 45:6999–7001. doi:0.1016/j.tetlet.2004.08.002
23. Frenkel D (2002) Understanding molecular simulation. Academic, San Diego, CA
24. Levitt M, Hirshberg M, Sharon R, Daggett V (1995) Potential energy function and parameters for simulations of the molecular dynamics of proteins and nucleic acids in solution. Comput Phys Commun 91:215–231. doi:10.1016/0010-4655(95)00049-L
25. Zhang D, Liu Z, Xu R (2007) Monte Carlo simulation of the adsorption of C_2-C_7 linear alkanes in aluminophosphate $AlPO_4$-11. Mol Sim 33:1247–1253. doi:10.1080/08927020701697683
26. Bezrodna T, Melnyk V, Vorobjev V, Puchkovska G (2010) Low-temperature photoluminescence of 5CB liquid crystal. J Luminescence 130:1134–1141. doi:10.1016/j.jlumin.2010.02.009
27. Kirkpatrick S, Gelatt CD, Vecchi MP (1983) Optimization by simulated annealing. Science 220:671–680. doi:10.1126/science.220.4598.671

28. Ju SP, Yang SH, Liao ML (2006) Study of molecular behavior in a water nanocluster: size and temperature effect. J Phys Chem B 110:9286–9290. doi:10.1021/jp056567p
29. Ju SP, Lin JS, Lee WJ (2004) A molecular dynamics study of the tensile behaviour of ultrathin gold nanowires. Nanotechnology 15:1221. doi:10.1088/0957-4484/15/9/019
30. Ju SP, Lee WJ, Lin JS, Liao ML (2006) Strain rate effect on tensile behavior of the helical multi-shell gold nanowires. Mater Chem Phys 100:48–53. doi:10.1016/j.matchemphys.2005.12.005
31. Rapaport DC (2004) The art of molecular dynamics simulations. Cambridge University Press, Cambridge, UK